Published online 15 November 2006 *Nucleic Acids Research, 2006, Vol. 34, No. 21* ***e144***
doi:10.1093/nar/gkl787

A microfluidic-FCS platform for investigation on the dissociation of Sp1-DNA complex by doxorubicin

Hsin-Chih Yeh[1], Christopher M. Puleo[2], Teck Chuan Lim[2], Yi-Ping Ho[1], Paul E. Giza[3], Ru Chih C. Huang[3] and Tza-Huei Wang[1,2,4,*]

[1]Department of Mechanical Engineering, [2]Department of Biomedical Engineering, [3]Department of Biology and [4]Whitaker Biomedical Engineering Institute, The Johns Hopkins University, Baltimore, MD 21218, USA

Received August 24, 2006; Revised September 19, 2006; Accepted September 28, 2006

ABSTRACT

The transcription factor (TF) Sp1 is a well-known RNA polymerase II transcription activator that binds to GC-rich recognition sites in a number of essential cellular and viral promoters. In addition, direct interference of Sp1 binding to DNA cognate sites using DNA-interacting compounds may provide promising therapies for suppression of cancer progression and viral replication. In this study, we present a rapid, sensitive and cost-effective evaluation of a GC intercalative drug, doxorubicin (DOX), in dissociating the Sp1–DNA complex using fluorescence correlation spectroscopy (FCS) in a microfluidic system. FCS allows assay miniaturization without compromising sensitivity, making it an ideal analytical method for integration of binding assays into high-throughput, microfluidic platforms. A polydimethylsiloxane (PDMS)-based microfluidic chip with a mixing network is used to achieve specific drug concentrations for drug titration experiments. Using FCS measurements, the IC_{50} of DOX on the dissociation of Sp1–DNA complex is estimated to be 0.55 μM, which is comparable to that measured by the electrophoretic mobility shift assay (EMSA). However, completion of one drug titration experiment on the proposed microfluidic-FCS platform is accomplished using only picograms of protein and DNA samples and less than 1 h total assay time, demonstrating vast improvements over traditional ensemble techniques.

INTRODUCTION

The transcription factor (TF) Sp1, a member of a large family of zinc finger proteins, was first identified in HeLa cells based on its ability to activate the SV40 early promoter (1,2). Subsequently, the ubiquitously expressed Sp1 has been indicated in transcriptional activation of a wide variety of genes through selective binding to a GC-rich DNA sequence (GC box). Furthermore, synergistic or direct interactions with several other TFs and cell-cycle regulatory proteins have revealed a complex role for Sp1 in mediation of transcription of many cellular genes during development (3,4) and of over-expressed genes during tumor growth (5,6). Still, previous studies have revealed that host Sp1 protein binding is critical for transcriptional regulation of several viral genes in both herpes simplex virus type 1 (HSV-1) and human immunodeficiency virus type 1 (HIV-1) (7,8). Not surprisingly, this information led to studies aimed at developing antitumoric and antiviral compounds designed to disrupt Sp1-dependent gene expression in cancerous and infected cells. Specifically, HIV replication in cultured cells was suppressed by using mutation-insensitive DNA-interacting drugs to inhibit HIV Tat transactivation by blocking Sp1 binding at GC boxes on the long terminal repeat (LTR) promoter (7,8). Similarly, growth arrest and cellular apoptosis of cancer cells were induced by inhibiting Sp1-dependent Cdc2 and survivin expression (5,6,9).

Mechanistically, these DNA-interacting drugs resemble TFs in their preference for DNA sequences and groove orientations and prevent formation of TF–DNA complexes either by directly competing with the TF for the same DNA sites or by indirectly inducing DNA conformational changes. Several studies have been carried out to evaluate the effects of DNA-interacting drugs as inhibitors of the Sp1–DNA complex using electrophoretic mobility shift assay (EMSA) coupled with radioactive-based detection (5–8,10–13). However, utilizing EMSA as the primary method of evaluating drug-induced disruption of TF–DNA complexes presents a number of drawbacks, including time-consumption, reagent-consumption, and lack of quantification. For example, in order to clearly resolve the bands in EMSA, several tens of nanograms of TF are needed to saturate binding sites on the nanograms of DNA required per well, thereby imposing a high reagent cost on this assay. These requirements make EMSA applicable only to abundantly expressed TFs. More

*To whom correspondence should be addressed. Tel: +1 410 516 7086; Fax: +1 410 516 7254; Email: thwang@jhu.edu

importantly, EMSA is not an equilibrium, homogeneous assay and TF–DNA complex disruption may occur due to the gel pore size and buffer conditions during electrophoresis, leading to underestimated protein binding activity (14–16). To overcome these and many more limitations, an assay that allows fast, accurate and reproducible determination of TF bindings at a single-molecule level is increasingly in demand.

Fluorescence-based methodologies, such as time-resolved fluorescence, fluorescence anisotropy, fluorescence resonance energy transfer (FRET), fluorescence intensity distribution analysis (FIDA) and fluorescence correlation spectroscopy (FCS), play an increasingly important role in allowing rapid and accurate determination of receptor-ligand binding fractions in an equilibrium, homogeneous and separation-free format (17–22). Unlike most of the fluorescence methods that are based on ensemble emission average, FCS is a technique that allows the fluorescence measurements to be carried out in a nanoscale domain with single-molecule resolution (23–29). In FCS measurements, the temporal fluctuations of fluorescence signal detected from fluorescent molecules diffusing through a femtoliter-sized detection volume are analyzed via an autocorrelation function, providing the kinetic information required to monitor changes in the molecular states and the concentration of fluorescent molecules (30–32). Due to the nature of the femtoliter-sized detection volume, FCS may allow miniaturization of assay volume without comprising assay sensitivity (19–22). Therefore, FCS is well suited to be incorporated in a microfluidic format, achieving rapid, highly sensitive and cost-effective analysis.

This report describes a binding assay platform that implements FCS on a microfluidic titration chip for the study of the displacement of Sp1 from the Sp1–DNA complex by a GC-intercalative agent, doxorubicin (DOX). The titration chip combines a microfluidic mixing network (33) with a valving system created using a multilayer soft lithography process (34–36) to generate drug solutions of varying concentrations; expose Sp1–DNA complexes to these drug dilutions; and separate each combination into nanoliter-sized interrogation chambers. Quantitative evaluation of Sp1-DNA binding inhibition by DOX is then accomplished by FCS measurements directly on the chip. In this report, we first characterize the FCS detection scheme in resolving the correct binding fractions of a controlled DNA binary-mixing system. The binding affinity (K_d) of the Sp1–DNA interaction (32 nM) is then discerned based on the same FCS analysis scheme. Second, FCS measurements are carried out inside polydimethylsiloxane (PDMS) microchambers containing 300 nl to 10 pl DNA samples to validate that FCS is indeed insensitive to miniaturized sample volumes. Third, a dose-response curve of DOX on Sp1-DNA inhibition is compiled using the proposed microfluidic-FCS platform and used to determine the concentration of DOX required to give 50% Sp1 binding inhibition (IC_{50}). The IC_{50} (0.55 μM) generated by the FCS measurements agrees well with the semi-quantitative EMSA data previously provided in literature (10). However, the advantages of this chip-based FCS technology are obvious. For example, drug titration on the microfluidic platform requires only 300 pg of Sp1 and 15 pg of DNA fragments, and the evaluation on drug potency is completed within 1 h.

MATERIALS AND METHODS

Oligonucleotides and Sp1

The DNA target for Sp1-binding experiments was a 23 bp DNA fragment [Cy5-ACTTTCCAGGGAGGCGTGGCCTG, M.W. 14.6 kDa, Sp1-binding site underlined (37,38)] spanning from −87 to −65 nt of the HIV LTR promoter (7,8). This dsDNA target was formed by annealing of two high performance liquid chromatography (HPLC)-purified synthetic ssDNA (Integrated DNA Technology), one of which was 5′-end labeled with a Cy5 dye. Hybridization was carried out in 5 mM Tris–HCl (pH 8.0) buffer where the temperature was slowly cooled down from 95°C to room temperature. The truncated Sp1 protein (M.W. 17 kDa) was overproduced from a bacterial Rop expression system that consisted of 530–685 amino acids of the C-terminal, three zinc-finger DNA-binding domains (1). The protein was purified to 95% homogeneity. The DNA binding capability of this completely refolded recombinant Sp1 was first verified using EMSA before further testing with the FCS system. The reason for using this truncated Sp1 was to allow a clear Sp1-DNA binding band in EMSA. Doxorubicin hydrochloride (Sigma–Aldrich, M.W. 580 Da) was prepared in dimethyl sulfoxide (DMSO) and stored at 4°C.

FCS setup

FCS measurements were carried out with a custom-built inverted confocal fluorescence spectroscope (39,40). A He-Ne (633 nm, 25-LHP-151-249, Melles Griot) laser was used to excite the Cy5 dyes. The laser beam was expanded to ∼5 mm in diameter by a telescope and was reflected by a dichroic mirror (51008 BS, Chroma Technology) into a microscope objective (100 × N.A. 1.3, oil immersion, UPlanFl, Olympus). Fluorescence emitted from the sample was collected with the same objective (epi-illumination) and passed though a 50 μm pinhole (PNH-50, Melles Griot) installed in an image plane of the microscope to eliminate out-of-focus signal. A band pass filter (670DF40, Omega Optical) was used to reduce the background signal and the filtered fluorescence light was then focused onto an avalanche photo diode (SPCM-AQR-13, PerkinElmer). The output electronic signal was fed into a correlator (ALV-5000/EPP, ALV-GmbH) to compute the autocorrelation functions. The power of the laser was adjusted to 100 μW by a neutral density filter before entering the objective. This power level resulted in good fluorescence signals, but was low enough to keep photobleaching of Cy5 negligible (41,42). The half radii of the detection volume were determined to be ∼0.4 μm in x-y and 4 μm in z directions, respectively, by fitting the autocorrelation function of free Cy5 in water, assuming a 3D Gaussian-shaped detection volume and a diffusion coefficient of $D = 2.5 \cdot 10^{-6}$ cm^2/s (41,43). The laser beam was focused 10 μm into the sample and was controlled by a piezo-actuator with sub-micron resolution (P-517.3CL, Physik Instrumente) for all FCS measurements in this report.

Analysis of FCS data

When only one type of fluorescent species is present, for instance, the labeled DNA alone, the analysis of the

autocorrelation curve is carried out with a least squares fit using the following one-component analytical model (41,44):

$$G(\tau) = \frac{1}{N} g_D(\tau) X(\tau) \quad \mathbf{1}$$

Here N is the average number of light-emitting particles diffusing in the detection volume and $g_D(\tau)$ is the autocorrelation function arising from fluorescence fluctuations due to translational diffusion. The analytical expression for $g_D(\tau)$ based on diffusion through a Gaussian-shaped detection volume often fits poorly to the experimental FCS curves, possibly due to spherical aberration of the objective or the distorted excitation profile resulted from the increased laser power (45,46). In order to account for these effects and to better fit the FCS curves, a semi-empirical expression, which has a form similar to that of anomalous diffusion inside living cells (47,48), is used here to describe $g_D(\tau)$:

$$g_D = \left(\frac{1}{1 + (\frac{\tau}{\tau_d})^{\alpha}} \right), \quad \mathbf{2}$$

where α is the anomalous factor. $X(\tau)$ represents the fluctuations in the fast time range due to triplet-state relaxation and *trans-cis* isomerization of Cy5 dye and is defined by (41,42):

$$X(\tau) = \frac{1 - F + Fe^{-\frac{\tau}{\tau_r}}}{1 - F} \quad \mathbf{3}$$

F is the fraction of molecules in non-fluorescent states and τ_r is the relaxation time.

In the presence of two types of fluorescence species, for instance, the free DNA and the Sp1-bound DNA, the molar fraction of the second species (e.g. the Sp1-bound DNA), Y, can be determined using the following two-component analytical model (19,23,44):

$$G(\tau) = \frac{1}{N}[(1 - Y) g_{F,D} X_F + YQ^2 g_{B,D} X_B], \quad \mathbf{4}$$

where Q is the relative brightness of the bound species compared to the free, unbound species. The subscripts F and B denote the free and bound species, respectively. The molar fraction of Sp1-bound DNA, Y, can also be regarded as the degree of binding in Sp1-DNA binding experiments. The least-squares fit used in this report is based on the Levenberg–Marquardt algorithm within Origin 7.0 (OriginLab).

Sp1-DNA binding experiments

Samples for Sp1-DNA binding experiments contained 5 nM Cy5-labeled dsDNA fragment and 10–120 nM truncated Sp1 in a buffer with 10 mM Tris–HCl (pH 7.5), 25 mM NaCl, 2.5 mM $MgCl_2$, 25 μM $ZnSO_4$, 0.05% NP-40, 7 mM 2-mercaptoethanol and 250 μg/ml BSA (1 × Sp1-DNA binding buffer). The reaction samples were incubated for 10 min at room temperature before FCS measurements. The diffusion times and other FCS parameters were first determined for the free DNA and DNA bound with Sp1 by saturating the DNA with a high concentration of Sp1. FCS parameters used in two-component analysis are listed in Table 1.

Table 1. Parameters used in two-component FCS analysis

	τ_d (μs)	F	τ_r (μs)	α	Q
(1) In DNA binary-mixing experiment:					
dsDNA	344	0.149	18	0.95	0.616
ssDNA	241	0.326	14	0.93	
(2) In Sp1-DNA binding experiment:					
DNA	344	0.149	18	0.95	0.719
Sp1-DNA	431	0.151	18	0.93	

Symbols: τ_d, diffusion time; F, fraction of fluorescent molecules in non-fluorescent states; τ_r, relaxation time; α, anomalous factor; Q, relative brightness.

Fabrication of microfluidic chips

Microfluidic titration chips were fabricated based on a multi-layer soft lithography process (34–36). Two layers of PDMS structures were constructed, one for sample delivery and processing and the other for mechanical on-off valving (Figure 1). For the sample delivery (fluidic) layer, SJR5740 (Shipley) was used as the mold material and was patterned in bas-relief on a 4″ silicon wafer using a standard photolithography process. After a reflow process at 180°C on a hotplate for 30 min, the resist mold had a semi-circular cross section (~15 μm tall). For the mechanical valving layer, SU-8 2025 (MicroChem) was used to make a 20 μm tall mold. PDMS prepolymer (mixing ratio = 1:7, Sylgard 184, Dow Corning) was cast on the SU-8 valve masters to reach a thickness of ~ 4 mm and cured thermally at 80°C in an oven for 9 min. Silicon wafers with SJR5740 channel molds were silanized in a desiccator with vapor of chlorotrimethylsilane (Sigma–Aldrich). PDMS prepolymer (mixing ratio 1:15) was spin-coated on the SJR5740 channel masters at 2000 rpm for 60 s, followed by a thermal curing at 85°C in an oven for 6 min. The cured PDMS sheet containing mechanical valves was first peeled away from the SU-8 silicon master and cut into a proper chip size. The hole for the valve control inlet was formed by punching through the PDMS sheet using a syringe needle (McMaster-Carr). This valve PDMS sheet was then placed on top of the cured PDMS fluidic layer, which was still on the SJR5740 silicon master. The two layers were fused together by baking the wafer at 85°C in an oven for 25 min. The fused PDMS sheets were peeled from the silicon master together and cut into proper chip size. The holes for the sample inlets and outlets were formed again using a syringe needle. The microfluidic chip was completed by plasma oxidation of the PDMS surface and irreversible sealing to a 170 μm-thick glass slide. The samples were delivered to the microfluidic chip via a 1 ml syringe and 0.02 inch I.D. Tygon® tubing (Cole-Parmer) fitted with 23-gauge steel needle tips (McMaster-Carr). The sample injection rate was controlled by a syringe pump (PHD 2000, Harvard Apparatus).

Separately, an array of microchambers of varying sizes for evaluating the performance of FCS in miniaturized assay volumes were patterned on a PDMS sheet using the above described SU-8 molding process. The DNA sample was sandwiched between a microscope slide and a patterned PDMS sheet containing various sized microchambers, following the procedure described by Rondelez *et al*. (49). Excess sample was squeezed out by applying pressure to the

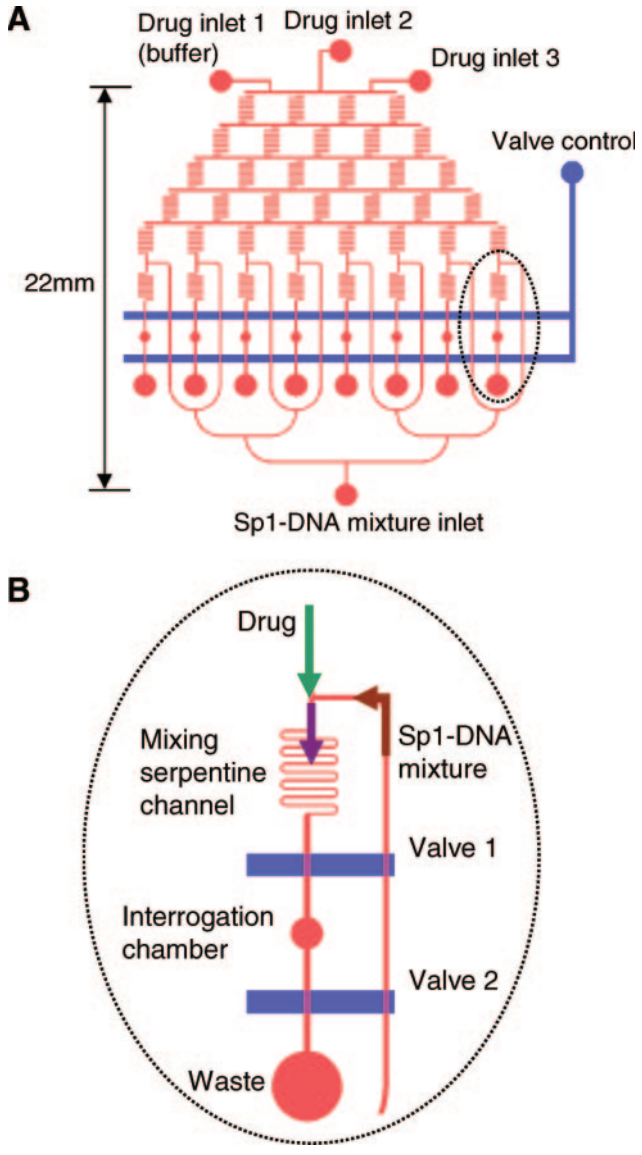

Figure 1. The PDMS-based microfluidic chip used for investigation on the dissociation of Sp1–DNA complex by DOX. (**A**) The layout of microchannels (red) and the mechanical on-off valves (blue). (**B**) A zoom-in of the mixing portion on the microfluidic chip: a serpentine channel is used for enhancing the mixing of the drug solution and the Sp1-DNA mixture. The interrogation chamber has the size of ~3 nl and can be isolated by simultaneously closing the two valves to stop the flow in microchannels.

PDMS sheet and the PDMS bonded to the cover slip by van der Waals forces.

Drug titration experiment on PDMS microfluidic chip

DOX solutions at three different concentrations were introduced to inlets on the upper part of the microfluidic titration chip (Figure 1) and the Sp1-DNA mixture was introduced to the single inlet on the lower part of the chip. The concentrations chosen for DOX injection were 0 (1 × Sp1-DNA binding buffer only), 40 nM and 4 μM, respectively. The Sp1-DNA mixture, which contained 10 nM DNA fragments and 160 nM Sp1, was incubated at room temperature for 10 min prior to injection into the microchannels, which were first flushed with 1 mg/ml BSA in HEPES buffer for 20 min to prevent protein adsorption on the PDMS surface (44,49,50). The diluted DOX solutions were then injected into the microchannels at a flow rate of 0.1 μl/min and the Sp1-DNA mixture was injected at a flow rate three times that of the DOX. The serpentine channels within the microfluidic network enhanced mixing either between the neighboring streams of the DOX solutions or between the diluted DOX solutions and the Sp1-DNA mixtures.

After samples within the mixing network reached a steady-state flow, the two mechanical valves were simultaneously turned on to 'close' the FCS interrogation chambers by applying ~ 20 psi of compressed air to the valve inlet (valves were primed with water), thus isolating the Sp1-DNA complexes mixed with various amounts of DOX in eight different interrogation chambers, each containing a volume of ~ 3 nl. After incubation for 10 min, FCS measurements were taken inside each of the eight microchambers.

Drug titration experiment using EMSA

A DOX titration experiment was carried out using EMSA as a proof to validate the proposed microfluidic-FCS platform. The reaction samples for EMSA contained 10 mM Tris–HCl (pH 7.5), 25 mM NaCl, 2.5 mM $MgCl_2$, 25 μM $ZnSO_4$, 0.05% NP-40, 7 mM 2-mercaptoethanol, 250 μg/ml BSA, 10% glycerol, 1 ng ^{32}P-labeled DNA fragment, and 20 ng Sp1 per each 15 μl reaction. DOX was added to the reaction to give an appropriate final DOX concentration for the reaction volume of 15 μl. After incubation for 10 min at room temperature, electrophoresis was performed in a 5% non-denaturing polyacrylamide gel using TBE buffer [89 mM Tris base, 89 mM boric acid and 1 mM EDTA (pH 8.0)] with each lane receiving 7 μl of each reaction volume.

RESULTS

FCS analysis for determining binding fractions

In order to evaluate the two-component analytical model (Equation 4) in determining molecular binding fractions, an experiment analyzing binary mixtures of labeled ssDNA and its dsDNA hybrid with FCS was performed. The 23 bp, Cy5-labeled dsDNA hybrid was mixed with the 23 nt, Cy5-labeled ssDNA (M.W. 7.6 kDa) to obtain different molar fractions of dsDNA to total DNA (R: [dsDNA]/([dsDNA]+[ssDNA])), simulating various binding fractions (Y: the fraction of Cy5-labeled DNA strand forming duplex). The total DNA concentration was fixed at 5 nM in each mixture and diffusion times (τ_d) and other FCS parameters (F, τ_r, α) were first determined using the one-component model (Equation 1) for samples containing only ssDNA or dsDNA (Table 1). The relative brightness (Q) of dsDNA to ssDNA was estimated to be 0.616 from fluorescence intensity analysis. These parameters were then used in the two-component model (Equation 4) to analyze the autocorrelation curves measured from the binary mixtures in order to derive Y in each sample. As shown in Figure 2A, the measured (Y) values agree well with the mixing (R) values, showing the high accuracy achieved by this two-component FCS analysis in

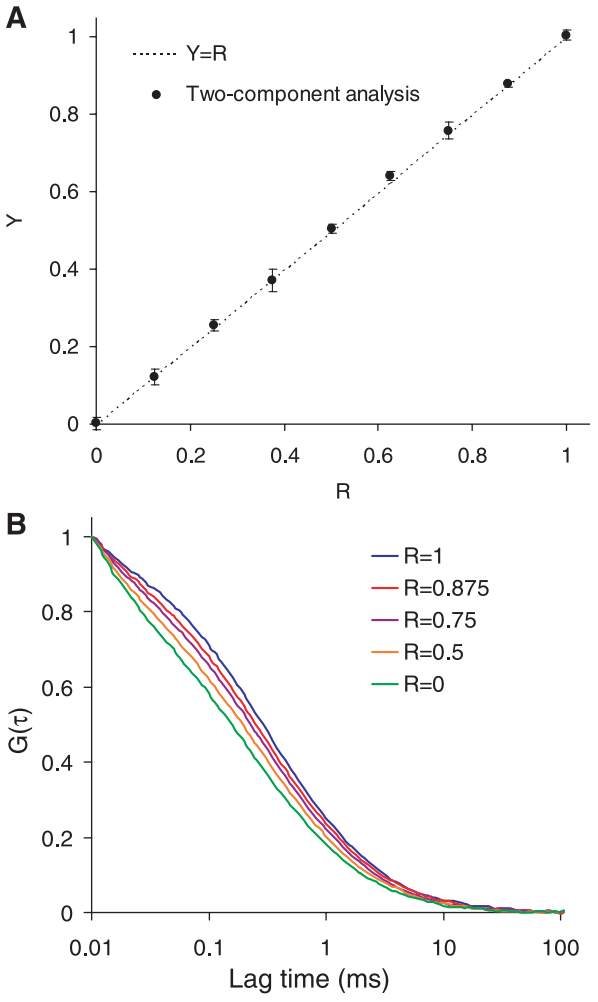

Figure 2. (**A**) Validation of the two-component FCS model using a DNA binary-mixing system. R: the mixing molar fraction of dsDNA to total DNA. Y: the measured molar fraction of Cy5-labeled DNA strand forming duplex. The dash line represents the situation of Y equal to R and the filled circles represent the measured Y at each R. Error bars represent standard deviations from six FCS measurements. (**B**) Normalized autocorrelation curves measured from five binary-mixing samples (R = 0, 0.5, 0.75, 0.875 and 1).

determining degrees of molecular bindings. Figure 2B shows the normalized autocorrelation curves measured from some of the binary-mixing samples.

Sp1-DNA binding affinity measurements

A titration experiment was performed to determine the binding affinity of Sp1 to its consensus DNA-binding site. Six 100-sec measurements were taken from 10 samples, which contained fixed amount of DNA fragments (5 nM) and various amounts of Sp1 (10–120 nM). The relative brightness (Q) of Sp1–DNA complex to free DNA was estimated to be 0.719 from fluorescence intensity analysis. The resulting binding fractions from two-component FCS analysis at each Sp1 concentration were plotted in Figure 3, which yields an affinity K_d of 32 ± 2 nM from a hyperbolic fit. This result is in good agreement with the affinity estimated from EMSA (51).

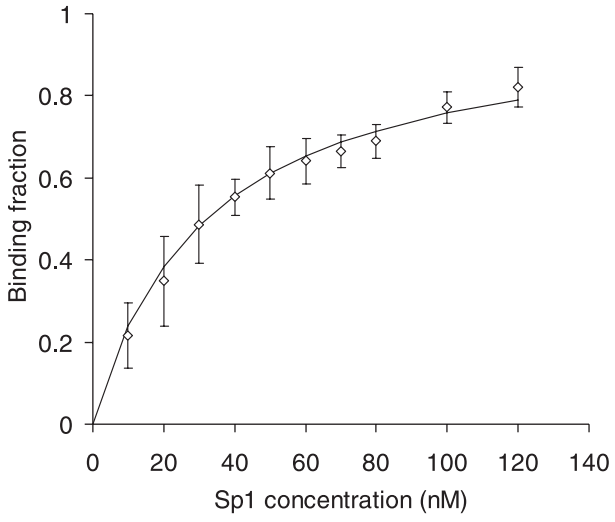

Figure 3. DNA-binding fractions at various Sp1 concentrations characterized by FCS measurements and the two-component analysis. The solid curve results from a hyperbolic fit, yielding a binding constant of $K_d = 32 \pm 2$ nM. Error bars represent standard deviations from six FCS measurements.

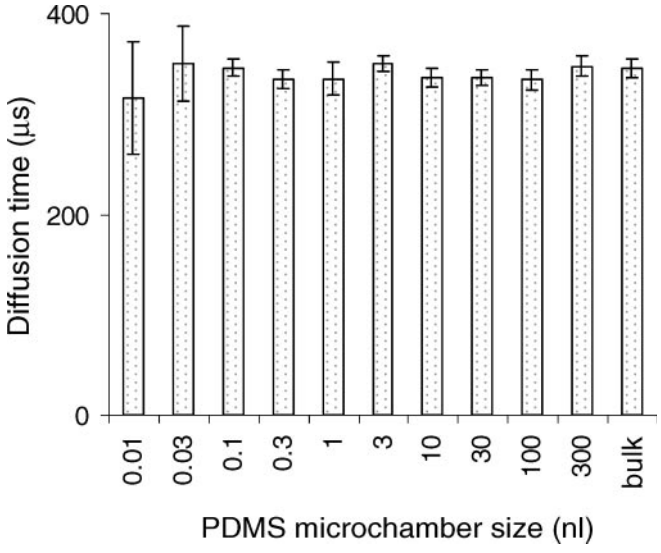

Figure 4. Diffusion times of the 23 bp DNA fragment measured using FCS in nanoliter to picoliter-sized microchambers. Bulk measurements are carried out in a 20 μl chambered glass plate. Error bars represent standard deviations from six FCS measurements.

FCS results versus assay volumes

To evaluate the potential of using FCS in miniaturized assay volumes, we performed FCS measurements in an array of PDMS microchambers of volumes decreasing from microliter to picoliter. Experiments were made to determine DNA diffusion times with FCS using a sample containing dsDNA fragments at 5 nM. As shown in Figure 4, the measured values of DNA diffusion times were found consistent despite decreasing assay volumes. The measured diffusion times remained nearly unchanged even when the chamber size was reduced down to 30 pl. Yet, when a chamber of 10 pl was used for measurements, a decreased diffusion time

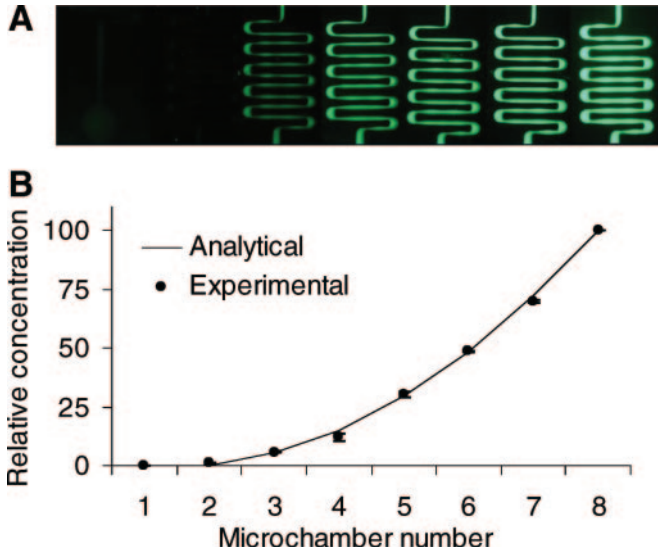

Figure 5. Characterization of concentration gradients generated by the Christmas tree-like microfluidic mixing network with three inlets at relative fluorophore concentrations of 0, 1 and 100. (**A**) Fluorescence micrographs of solution gradients of fluorescein at serpentine mixing channel regions. (**B**) Concentration gradients determined from analytical model (−) and from single-molecule counting (•). Error bars represent standard deviations from four measurements.

accompanied by an increased deviation was noted, possibly due to interference of the illumination and collection light paths from the small chamber opening at this volume scale. This result demonstrates that FCS assays are well suited for assay miniaturization and can be performed at an assay volume of sub-nanoliter or smaller without compromising analysis integrity.

Drug evaluation using FCS on titration chip

We incorporated a design using triple inlets in the microfluidic mixing network for the titration experiment as this design allowed generation of varying concentrations of analyte spanning nearly three orders of magnitude in the outlet channels (33). The length of the serpentine channels (10 mm) was sufficiently long to allow full mixing of the neighboring fluid streams, given the flow speed of drug solutions (~3 mm/s) and the estimated diffusion coefficient of the drug ($\sim 5 \cdot 10^{-6}$ cm^2/s). The relative concentrations in the downstream channels were measured through fluorescence imaging with high-concentration fluorescein and through single-molecule counting with low-concentration Cy5 dyes (Figure 5A and 5B), which both showed good agreement with the analytical result calculated based on the scheme described in literature (33). For the DOX titration experiment, eight different DOX solutions of varying concentrations were generated in the downstream channels (0, 11.7 nM, 214 nM, 604 nM, 1.18 μM, 1.94 μM, 2.88 μM and 4 μM, respectively) when introducing three DOX solutions at concentrations of 0, 40 nM and 4 μM. After mixing with the incoming solutions of Sp1-DNA mixtures at a controlled flow rate, the final concentration of DOX in the eight interrogation chambers were 0, 5.9 nM, 107 nM, 302 nM, 0.59 μM, 0.97 μM, 1.44 μM and 2 μM, while the

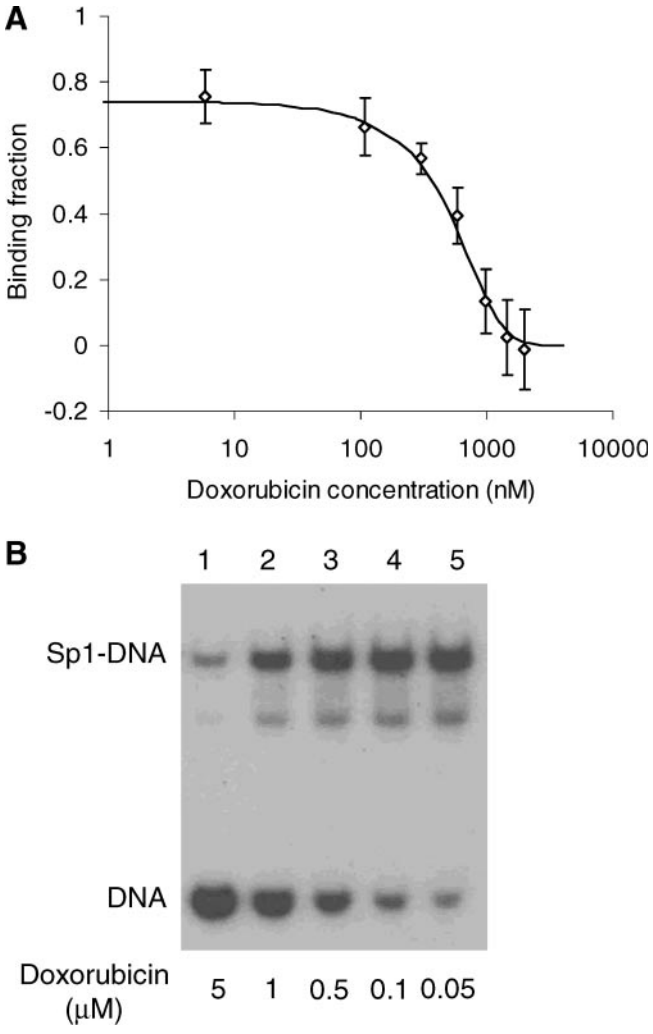

Figure 6. (**A**) The dose-response titration curve of DOX on the dissociation of Sp1–DNA complex. FCS measurements are carried out on a PDMS titration chip. IC_{50}, the DOX concentration required to give 50% Sp1 binding inhibition, is estimated to be 0.55 μM. Error bars represent standard deviations from five FCS measurements. (**B**) Dox titration experiment using EMSA. The gel result also indicates the IC_{50} around 0.5 μM.

concentrations of Sp1 and DNA were 80 and 5 nM, respectively. Figure 6A shows the dose-response curve of DOX in the Sp1-DNA inhibition experiment. The IC_{50} of DOX on the dissociation of Sp1–DNA complex, derived from a dose-response fit of the binding curve, was determined to be 0.55 μM, which was comparable to that derived from the EMSA result (Figure 6B) and the value reported in literature (10).

DISCUSSION

Fast and cost-effective means of characterizing drug-target interactions is of considerable importance in pharmaceutical discovery. To address this requirement, we have developed a semi-automatic titration platform for mechanistic analysis of drug–protein–DNA interactions by implementing a rapid FCS detection scheme in a low-volume, microfluidic format. We have demonstrated that FCS was insensitive to assay

miniaturization and have shown consistent measurement results of diffusion times when reducing the assay volume down to the sub-nanoliter regime. In the current titration experiment, the total volume of reagents required for filling the microchannels and the interrogation chambers on the chip are ~300 nl for drug solutions and ~100 nl for Sp1-DNA mixture. As a result, this experiment consumes only 300 pg of Sp1 and 15 pg of DNA, as opposed to hundreds of nanograms of protein and DNA that are required by conventional EMSA (7,8,10,11). In addition, the overall assay time of the microfluidic FCS platform is much shorter than that of EMSA (~10 h) and the results are more quantitative due to the large amount of parameters and kinetic data acquired in the FCS measurements. Further reduction in reagent consumption per assay can be achieved by using a titration chip that incorporates interrogation chambers of further reduced sizes and allows automatic multiplexed assays with shared fluid inputs and delivery channels. Further reduction in run time can also be achieved by using a highly integrated FCS setup with parallel detection capability (52).

A commonly cited disadvantage of using FCS for binding assay is the requirement of at least 5-to 8-fold increase in mass (19,53) or 1.6-fold increase in diffusion time (44) on binding in order to clearly differentiate the unbound species from the bound one. In this report, we achieve for the first time using FCS in differentiating between a ssDNA (M.W. 7.3 kDa) and its dsDNA hybrid (M.W. 14.6 kDa) in solutions. When measuring their binary mixtures, the error between the measured molar fraction, Y, and the mixing molar fraction, R, is found to be less than 0.02 (Figure 2A). Similar results have been demonstrated when analyzing Sp1-DNA binding, where the binding-induced mass increase is only 2.16 fold. Multiple experimental factors are thought to contribute to this expansion of previously cited limits of FCS as an analytical technique. First, FCS measurements are strongly weighed in favor of the brighter component (e.g. the unbound species) and the proper selection of relative brightness, Q, in two-component FCS analysis (Equation 4) is critical in order to obtain precise binding fractions (see Supplementary Data) (19,23,44). Second, as aforementioned, a semi-empirical expression for $g_D(\tau)$ (Equation 2) is used to better fit the experimental FCS curves, allowing more accurate binding fraction analysis and resulting in a smaller standard deviation among measurements (data not shown). Similar strategies using different $g_D(\tau)$ expressions are also seen in literature (45,46). Third, the fast-relaxation processes [$X(\tau)$, Equation 3] of Cy5 dye contribute to an additional shoulder in the microsecond region of the FCS curve. Due to variation in the fractions of fluorescent molecules in non-fluorescent states (F, see Table 1), the shape of this fast-relaxation shoulder in Cy5-ssDNA autocorrelation curve looks different from that in Cy5-dsDNA curve. This is believed to enlarge the 'window' between the two FCS single-species curves (Figure 2B), leading to a more accurate binding fraction determination. However, in the case of Sp1-DNA binding, the F value stays almost unchanged for the bound species. This is believed to result in a larger standard deviation in the Sp1 binding system (Figure 3) compared to that in the DNA binary-mixing system (Figure 2A). In addition, the reliability of FCS measurements is found to be improved by using Cy5, possibly due to the very low autofluorescence background signal from solvent near the Cy5 emission wavelengths.

Variations of the microfluidic network used in this report have been utilized previously in literature for generating multiple concentrations of biomolecules for use in biomedical assays and applications (54,55). By combining a microfluidic mixing network with a downstream valving system, fabricated using a multilayer soft lithography process, we have made a novel titration chip for analysis of drug-target interaction with FCS. The valve design allows isolation of samples inside a nanoliter-sized interrogation chamber and facilitates the kinetic study of molecules in a purely diffusion-governed environment. Surface adsorption of assay reagents to device materials is a complication unique to microfluidic-based assays and arises due to the skewed surface-to-volume ratios within microdevices compared to their macroscopic counterparts (49). However, this surface adsorption issue can be resolved by surface blocking rinses (1 mg/ml BSA in HEPES buffer) prior to use, ensuring a bioassay-compatible microfluidic device.

The generally accepted Sp1 core consensus site as proposed by Kadonaga *et al*. is GGGCGG (1). However, slight differences in recognition sequences for Sp1 that lack the core consensus but retain function are often seen in various promoter regions. GGGAGG is one of such sequences found in cardiac actin promoter (37) and HIV LTR promoter (8). Both of our EMSA and FCS results indicate that Sp1 bound strongly to this GGGAGG site, agreeing with the reports from other laboratories (8,37,38). Non-covalently binding drugs interact with DNA in one of two ways as intercalative agents, such as DOX described in the present study or as minor and/or major groove binders (10,13). Kinetics and modes of the binding by these two types of drugs are different. Beyond the model type of study, the proposed microfluidic-FCS platform may also be applied to investigate the binding of Sp1 or other TFs to different DNA-binding sites and possibly to examine the interaction of groove-binding drugs to DNA targets directly. Finally, the microfluidic-FCS method presents a versatile technology platform and in addition to the study of drug–protein–DNA interactions exemplified in this report, this new platform can be generally applied to study other types of molecular bindings, such as protein–ligand and protein–protein interactions.

SUPPLEMENTARY DATA

Supplementary Data are available at NAR online.

ACKNOWLEDGEMENTS

The authors like to thank R. Sova, and X. Wu for invaluable discussion and the material support. This work was supported by NSF and the Whitaker Foundation. Funding to pay the Open Access publication charges for this article was provided by NSF.

Conflict of interest statement. None declared.

REFERENCES

1. Kadonaga,J.T., Carner,K.R., Masiarz,F.R. and Tijian,R. (1987) Isolation of cDNA-encoding transcription factor Sp1 and functional-analysis of the DNA-binding domain. *Cell*, **51**, 1079–1090.

2. Dynan,W.S. and Tjian,R. (1983) Isolation of transcription factors that discriminate between different promoters recognized by RNA polymerase-Ii. *Cell*, **32**, 669–680.
3. Jeang,K.T., Chun,R., Lin,N.H., Gatignol,A., Glabe,C.G. and Fan,H. (1993) *In vitro* and *in vivo* binding of human-immunodeficiency-virus type-1 tat protein and Sp1 transcription factor. *J. Virol.*, **67**, 6224–6233.
4. Loregian,A., Bortolozzo,K., Boso,S., Sapino,B., Betti,M., Biasolo,M.A., Caputo,A. and Palu,G. (2003) The Sp1 transcription factor does not directly interact with the HIV-1 Tat protein. *J. Cell. Physiol.*, **196**, 251–257.
5. Chang,C.C., Heller,J.D., Kuo,J. and Huang,R.C.C. (2004) Tetra-O-methyl nordihydroguaiaretic acid induces growth arrest and cellular apoptosis by inhibiting Cdc2 and survivin expression. *Proc. Natl Acad. Sci. USA*, **101**, 13239–13244.
6. Park,R., Chang,C.C., Liang,Y.C., Chung,Y., Henry,R.A., Lin,E., Mold,D.E. and Huang,R.C.C. (2005) Systemic treatment with tetra-O-methyl nordihydroguaiaretic acid suppresses the growth of human xenograft tumors. *Clin. Cancer Res.*, **11**, 4601–4609.
7. Huang,R.C.C., Li,Y., Giza,P.E., Gnabre,J.N., Abd-Elazem,I.S., King,K.Y. and Hwu,J.R. (2003) Novel antiviral agent tetraglycylated nordihydroguaiaretic acid hydrochloride as a host-dependent viral inhibitor. *Antiviral Res.*, **58**, 57–64.
8. Gnabre,J.N., Brady,J.N., Clanton,D.J., Ito,Y., Dittmer,J., Bates,R.B. and Huang,R.C.C. (1995) Inhibition of human-immunodeficiency-virus type-1 transcription and replication by DNA sequence-selective plant lignans. *Proc. Natl Acad. Sci. USA*, **92**, 11239–11243.
9. Heller,J.D., Kuo,J., Wu,T.C., Kast,W.M. and Huang,R.C.C. (2001) Tetra-O-methyl nordihydroguaiaretic acid induces G(2) arrest in mammalian cells and exhibits tumoricidal activity *in vivo*. *Cancer Res.*, **61**, 5499–5504.
10. Chiang,S.Y., Azizkhan,J.C. and Beerman,T.A. (1998) A comparison of DNA-binding drugs as inhibitors of E2F1- and Sp1-DNA complexes and associated gene expression. *Biochemistry*, **37**, 3109–3115.
11. Park,R., Giza,P.E., Mold,D.E. and Huang,R.C.C. (2003) Inhibition of HSV-1 replication and reactivation by the mutation-insensitive transcription inhibitor tetra-O-glycyl-nordihydroguaiaretic acid. *Antiviral Res.*, **58**, 35–45.
12. Czyz,M. and Gniazdowski,M. (1998) Actinomycin D specifically inhibits the interaction between transcription factor Sp1 and its binding site. *Acta Biochimica Polonica*, **45**, 67–73.
13. Gniazdowski,M., Denny,W.A., Nelson,S.M. and Czyz,M. (2003) Transcription factors as targets for DNA-interacting drugs. *Curr. Med. Chem.*, **10**, 909–924.
14. Benotmane,A.M., Hoylaerts,M.F., Collen,D. and Belayew,A. (1997) Nonisotopic quantitative analysis of protein-DNA interactions at equilibrium. *Anal. Biochem.*, **250**, 181–185.
15. Hill,J.J. and Royer,C.A. (1997) Fluorescence approaches to study of protein-nucleic acid complexation. In Abelson,J.N. and Simon,M.I. (eds), *Fluorescence Spectroscopy Methods in Enzymology*. Academic Press Inc., San Diego, USA, Vol. 278, pp. 390–416.
16. Heyduk,T. and Lee,J.C. (1990) Application of fluorescence energy-transfer and polarization to monitor *Escherichia coli* camp receptor protein and lac promoter interaction. *Proc. Natl Acad. Sci. USA*, **87**, 1744–1748.
17. Rudiger,M., Haupts,U., Moore,K.J. and Pope,A.J. (2001) Single-molecule detection technologies in miniaturized high throughput screening: binding assays for G protein-coupled receptors using fluorescence intensity distribution analysis and fluorescence anisotropy. *J. Biomol. Screening*, **6**, 29–37.
18. Haupts,U., Rudiger,M., Ashman,S., Turconi,S., Bingham,R., Wharton,C., Hutchinson,J., Carey,C., Moore,K.J. and Pope,A.J. (2003) Single-molecule detection technologies in miniaturized high-throughput screening: fluorescence intensity distribution analysis. *J. Biomol. Screening*, **8**, 19–33.
19. Pope,A.J., Haupts,U.M. and Moore,K.J. (1999) Homogeneous fluorescence readouts for miniaturized high-throughput screening: theory and practice. *Drug Discovery Today*, **4**, 350–362.
20. Auer,M., Moore,K.J., Meyer-Almes,F.J., Guenther,R., Pope,A.J. and Stoeckli,K.A. (1998) Fluorescence correlation spectroscopy: lead discovery by miniaturized HTS. *Drug Discovery Today*, **3**, 457–465.
21. Moore,K.J., Turconi,S., Ashman,S., Ruediger,M., Haupts,U., Emerick,V. and Pope,A.J. (1999) Single molecule detection technologies in miniaturized high throughput screening: fluorescence correlation spectroscopy. *J. Biomol. Screening*, **4**, 335–353.
22. Haupts,U., Rudiger,M. and Pope,A.J. (2000) Macroscopic versus microscopic fluorescence techniques in (ultra)-high-throughput screening. *Drug Discovery Today*, **1**, 3–9.
23. Rauer,B., Neumann,E., Widengren,J. and Rigler,R. (1996) Fluorescence correlation spectrometry of the interaction kinetics of tetramethylrhodamin alpha-bungarotoxin with Torpedo californica acetylcholine receptor. *Biophys. Chem.*, **58**, 3–12.
24. Palo,K., Metz,U., Jager,S., Kask,P. and Gall,K. (2000) Fluorescence intensity multiple distributions analysis: concurrent determination of diffusion times and molecular brightness. *Biophys. J.*, **79**, 2858–2866.
25. LeCaptain,D.J., Michel,M.A. and Van Orden,A. (2001) Characterization of DNA–protein complexes by capillary electrophoresis-single molecule fluorescence correlation spectroscopy. *Analyst*, **126**, 1279–1284.
26. Zhong,Z.H., Pramanik,A., Ekberg,K., Jansson,O.T., Jornvall,H., Wahren,J. and Rigler,R. (2001) Insulin binding monitored by fluorescence correlation spectroscopy. *Diabetologia*, **44**, 1184–1188.
27. Sevenich,F.W., Langowski,J., Weiss,V. and Rippe,K. (1998) DNA binding and oligomerization of NtrC studied by fluorescence anisotropy and fluorescence correlation spectroscopy. *Nucleic Acids Res.*, **26**, 1373–1381.
28. Clamme,J.P., Azoulay,J. and Mely,Y. (2003) Monitoring of the formation and dissociation of polyethylenimine/DNA complexes by two photon fluorescence correlation spectroscopy. *Biophys. J.*, **84**, 1960–1968.
29. Christoph,S. and Meyer-Almes,F.J. (2003) Novel fluorescence based receptor binding assay method for receptors lacking ligand conjugates with preserved affinity: study on estrogen receptor alpha. *Biopolymers*, **72**, 256–263.
30. Schwille,P., MeyerAlmes,F.J. and Rigler,R. (1997) Dual-color fluorescence cross-correlation spectroscopy for multicomponent diffusional analysis in solution. *Biophys. J.*, **72**, 1878–1886.
31. Eigen,M. and Rigler,R. (1994) Sorting single molecules—application to diagnostics and evolutionary biotechnology. *Proc. Natl Acad. Sci. USA*, **91**, 5740–5747.
32. Kinjo,M. and Rigler,R. (1995) Ultrasensitive hybridization analysis using fluorescence correlation spectroscopy. *Nucleic Acids Res.*, **23**, 1795–1799.
33. Dertinger,S.K.W., Chiu,D.T., Jeon,N.L. and Whitesides,G.M. (2001) Generation of gradients having complex shapes using microfluidic networks. *Anal. Chem.*, **73**, 1240–1246.
34. Hong,J.W. and Quake,S.R. (2003) Integrated nanoliter systems. *Nat. Biotechnol.*, **21**, 1179–1183.
35. Unger,M.A., Chou,H.P., Thorsen,T., Scherer,A. and Quake,S.R. (2000) Monolithic microfabricated valves and pumps by multilayer soft lithography. *Science*, **288**, 113–116.
36. Xia,Y.N. and Whitesides,G.M. (1998) Soft lithography. *Angew. Chem., Int. Ed.*, **37**, 551–575.
37. Gustafson,T.A. and Kedes,L. (1989) Identification of multiple proteins that interact with functional regions of the human cardiac alpha-actin promoter. *Mol. Cell. Biol.*, **9**, 3269–3283.
38. Taylor,A., Webster,K.A., Gustafson,T.A. and Kedes,L. (1997) The anti-cancer agent distamycin A displaces essential transcription factors and selectively inhibits myogenic differentiation. *Mol. Cell Biochem.*, **169**, 61–72.
39. Yeh,H.C., Ho,Y.P., Shih,I.M. and Wang,T.H. (2006) Homogeneous point mutation detection by quantum dot-mediated two-color fluorescence coincidence analysis. *Nucleic Acids Res.*, **34**, e35.
40. Zhang,C.Y., Yeh,H.C., Kuroki,M.T. and Wang,T.H. (2005) Single-quantum-dot-based DNA nanosensor. *Nature Mater.*, **4**, 826–831.
41. Widengren,J. and Schwille,P. (2000) Characterization of photoinduced isomerization and back-isomerization of the cyanine dye Cy5 by fluorescence correlation spectroscopy. *J. Phys. Chem. A*, **104**, 6416–6428.
42. Widengren,J., Schweinberger,E., Berger,S. and Seidel,C.A.M. (2001) Two new concepts to measure fluorescence resonance energy transfer via fluorescence correlation spectroscopy: theory and experimental realizations. *J. Phys. Chem. A*, **105**, 6851–6866.

43. Lenne,P.F., Colombo,D., Giovannini,H. and Rigneault,H. (2002) Flow profiles and directionality in microcapillaries measured by fluorescence correlation spectroscopy. *Single Mol.*, **3**, 194–200.
44. Meseth,U., Wohland,T., Rigler,R. and Vogel,H. (1999) Resolution of fluorescence correlation measurements. *Biophys. J.*, **76**, 1619–1631.
45. Widengren,J., Mets,U. and Rigler,R. (1995) Fluorescence correlation spectroscopy of triplet-states in solution–a theoretical and experimental-study. *J. Phys. Chem.*, **99**, 13368–13379.
46. Van Orden,A. and Keller,R.A. (1998) Fluorescence correlation spectroscopy for rapid multicomponent analysis in a capillary electrophoresis system. *Anal. Chem.*, **70**, 4463–4471.
47. Schwille,P., Korlach,J. and Webb,W.W. (1999) Fluorescence correlation spectroscopy with single-molecule sensitivity on cell and model membranes. *Cytometry*, **36**, 176–182.
48. Banks,D.S. and Fradin,C. (2005) Anomalous diffusion of proteins due to molecular crowding. *Biophys. J.*, **89**, 2960–2971.
49. Rondelez,Y., Tresset,G., Tabata,K.V., Arata,H., Fujita,H., Takeuchi,S. and Noji,H. (2005) Microfabricated arrays of femtoliter chambers allow single molecule enzymology. *Nat. Biotechnol.*, **23**, 361–365.
50. Ostuni,E., Kane,R., Chen,C.S., Ingber,D.E. and Whitesides,G.M. (2000) Patterning mammalian cells using elastomeric membranes. *Langmuir*, **16**, 7811–7819.
51. Dohm,J.A., Hsu,M.H., Hwu,J.R., Huang,R.C.C., Moudrianakis,E.N., Lattman,E.E. and Gittis,A.G. (2005) Influence of ions, hydration, and the transcriptional inhibitor P4N on the conformations of the Sp1 binding site. *J. Mol. Biol.*, **349**, 731–744.
52. Blom,H. and Gosch,M. (2004) Parallel confocal detection of single biomolecules using diffractive optics and integrated detector units. *Curr. Pharm. Biotechnol.*, **5**, 231–241.
53. Mayboroda,O.A., van Remoortere,A., Tanke,H.J., Hokke,C.H. and Deelder,A.M. (2004) A new approach for fluorescence correlation spectroscopy (FCS) based immunoassays. *J. Biotechnol.*, **107**, 185–192.
54. Jiang,X.Y., Ng,J.M.K., Stroock,A.D., Dertinger,S.K.W. and Whitesides,G.M. (2003) A miniaturized, parallel, serially diluted immunoassay for analyzing multiple antigens. *J. Am. Chem. Soc.*, **125**, 5294–5295.
55. Pihl,J., Sinclair,J., Sahlin,E., Karlsson,M., Petterson,F., Olofsson,J. and Orwar,O. (2005) Microfluidic gradient-generating device for pharmacological profiling. *Anal. Chem.*, **77**, 3897–3903.